

STUDY OF *In-silico* ADMET, MOLECULAR DOCKING, AND STABILITY POTENTIAL OF SYNTHESIZED NOVEL TETRAZOLE BEARING CURCUMIN DERIVATIVES AND EVALUATION OF THEIR ANTICANCER POTENTIAL ON PANC-1 CELL LINES

Geeta Krishnamurthy¹, Lairikyengbam Deepti Roy¹, Jyotsna Kumar^{1,✉},
Pooja Gour¹, Shivanjali Esther Arland¹, Manikanda Prabu¹, Srinivasa GR,²
and Shreenivas MT²

¹Department of Chemistry, M. S. Ramaiah University of Applied Sciences, Bangalore-560058,
(Karnataka) India

²Honeychem Pharma Research Pvt. Ltd., Bangalore-560058, (Karnataka) India

✉Corresponding Author: drkumarchem111@gmail.com

ABSTRACT

Amplified expression of mutations in proteins is an important hallmark of malignant cancer. In all *RAS*-mutant human cancers, pancreatic ductal adenocarcinoma (PDAC) is considered the most *RAS*-fanatic cancer, with a frequency of 100% *KRAS* (Kirsten rat sarcoma virus) mutation. In the present work, curcumin, a dietary phytochemical, was used to design a series of novel curcumin analogues aiming to regulate *KRAS* protein. The molecular docking study revealed the ligand efficacy and binding affinity of designed curcumin analogues against target proteins. Drug-like behaviour and ADMET (absorption, distribution, metabolism, excretion, and toxicity) prediction of identified molecules were done, and most of the pharmacokinetic parameters were found to be quite satisfactory and within an acceptable range. Three of the most potent drug candidates have been synthesized and characterized by FTIR, ¹HNMR, and LC-MS spectral analysis. Results of the *in vitro* anti-proliferative activities of curcumin analogues showed persuasive anticancer activity against the PANC-1 cell lines. The present study will be helpful in exploring the new series of cogent curcumin analogues as anticancer agents.

Keywords: Curcumin, Tetrazole, *KRAS* Proteins, MTT Assay, Curcumin Analogues.

RASAYAN J. Chem., Vol. 16, No.1, 2023

INTRODUCTION

Cancer is the second most lethal disease that has spread worldwide. According to statistics, pancreatic cancer is the fourth most common cancer cause of death in 2021.¹ Any flaw in the signaling pathways disrupts normal growth regulation, resulting in cancer. Many therapies for different cancers are being used, which mainly interfere with different signaling pathways that involve *RAS* proteins.^{2,3} *KRAS* proteins, one of the members of the *RAS* family, pass on signals from outside the cell to the nucleus.⁴ Mutated *KRAS* proteins have all of the characteristics of cancer, such as proliferation, evasion of apoptosis, reprogrammed cell metabolism, angiogenesis, and invasion, followed by metastasis. Oncogenic *KRAS* is reported to be the driving force behind pancreatic ductal adenocarcinoma.⁵⁻⁸ In general, gemcitabine and doxorubicin-based chemotherapy are used for the treatment of patients with progressive pancreatic cancer, which is always associated with drastic side effects and a poor survival rate. Hence, to improve the survival rate of pancreatic cancer patients, researchers tried many ways, such as combinatorial approaches, conventional therapies, the usage of natural products, etc. Eccentric therapy involves the use of naturally occurring plant products for the treatment of cancer patients, which are commonly used in many conformists' food preparation and traditional medicines. As per the studies, it is estimated that around 50-74% of anticancer drugs are either derivatives of natural products or stimulated by natural compounds.^{9,10} One such naturally occurring polyphenolic compound is curcumin, derived from *Curcuma longa* (commonly known as

turmeric). Preclinical studies *in vitro* and *in vivo* have validated the wide therapeutic spectrum of curcumin's anti-inflammatory, antioxidant, antibacterial, antifungal, anticancer activities, etc., including its advantages of minimal side effects and low toxicity.^{9,10} Tetrazole core (Fig.-1) is being used for the making of drugs for fungal treatment, hypertension, tuberculosis, leishmaniasis, etc.¹¹ The resonance of double bonds in tetrazole systems causes charge delocalization, making them suitable hydrogen bond donors or acceptors.¹² Enhanced delocalisation of charge and better membrane penetration provides a prolonged half-life for the tetrazole group. The high density of nitrogen in tetrazole offers an opportunity to form hydrogen bonds, or Π -bond stacking, with the receptor site. As a result, increased binding affinity identifies tetrazole as having drug-like properties, making it more suitable for drug formulation.¹³ After the extensive literature review, the authors perceived that scanty papers reported the synthesis of curcumin analogues with tetrazole to study their anticancer activity. Hence, the authors designed a novel scaffold of curcumin analogues comprising a heterocyclic moiety. To extend the planned study and investigate the ADMET and anticancer activity, novel curcumin analogues, including the tetrazole moiety, were developed. The docking scores and binding abilities of designed curcumin analogues with the target protein KRAS (PDB code: 4EPV) were determined using virtual screening. Among 15 designed and screened curcumin analogues, molecular docking results identified three hit molecules with high docking scores. The ADMET properties were predicted to study their bioavailability and toxicity. These three hit molecules were further synthesized, and their identities were confirmed using ^1H NMR, LCMS, and FTIR. The anticancer activity of the three synthesized screened molecules was assessed by MTT assay on PANC-1 cell lines.

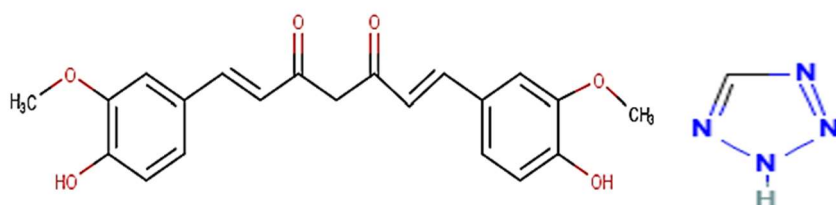


Fig.-1: Structure of Curcumin and Tetrazole Core

EXPERIMENTAL

Material and Methods

AR-grade chemicals of 98% purity were purchased from Sigma Aldrich and used without further purification. Drug likeness and molecular properties of novel curcumin analogues were anticipated using Molinspiration software, Swiss ADME, ADMETlab, and Syntell software. ^1H NMR analysis was carried out by a Bruker AV-III-400MHz NMR spectrometer, LC-MS was done on the Shimadzu LC-40 HPLC System, IR spectroscopy was done with the Nicolet iS20 FTIR Spectrometer from Thermo Fisher Scientific™ and the UV-2600 (UV-VIS Spectrophotometer from Shimadzu) was used for stability test of the synthesized drug molecules. Other instruments used were a rotavapor for concentration, a hot air oven for drying, and a magnetic stirrer with a heater for refluxing. For anticancer activity PANC-1 cell lines (Pancreas), Fetal bovine serum (FBS): Cat No; 10270106 (Gibco, Invitrogen), Dulbeccos Modified Eagle Media (DMEM) with low glucose: Cat No; 11965-092 (Gibco, Invitrogen), Antibiotic–Antimycotic 100X solution (Thermofisher Scientific) -Cat No-15240062 were used.

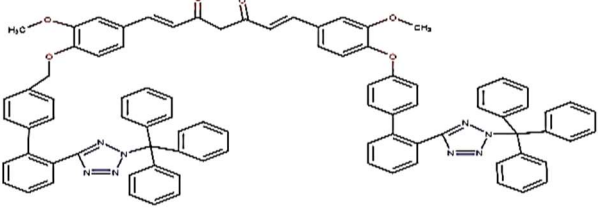
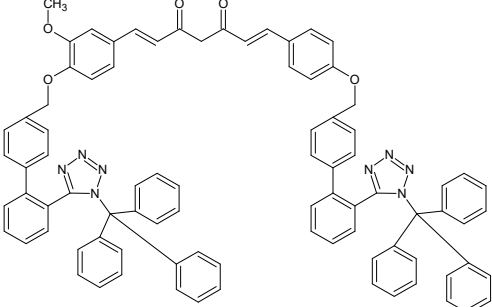
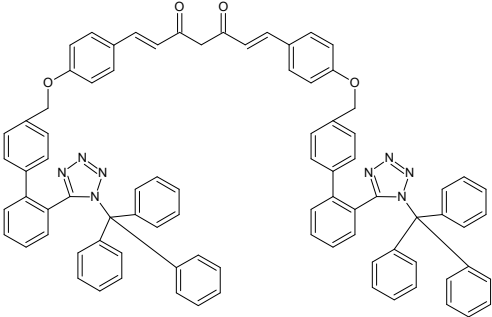
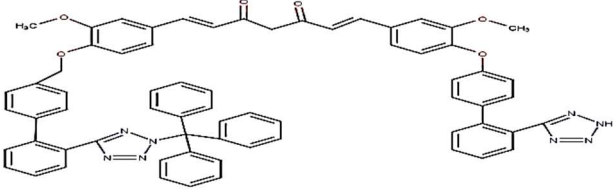
General Procedure

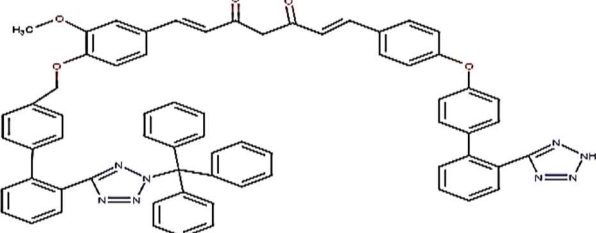
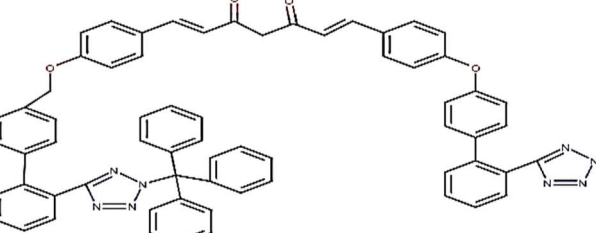
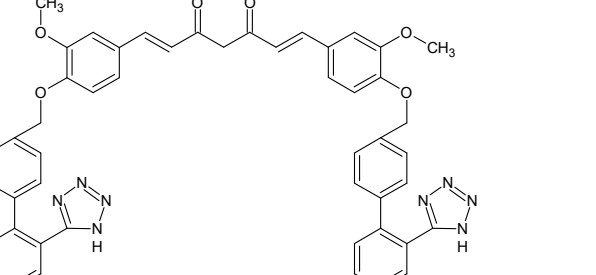
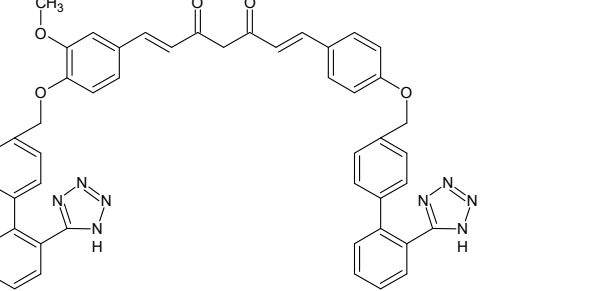
Computational Methodology: Ligand Preparation

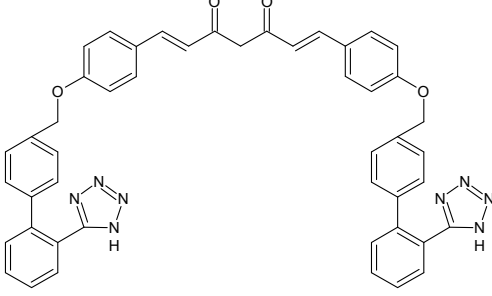
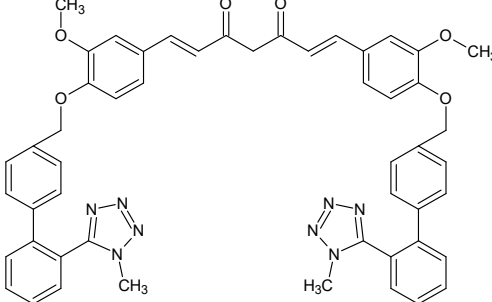
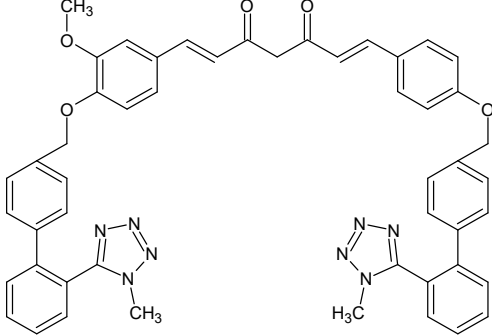
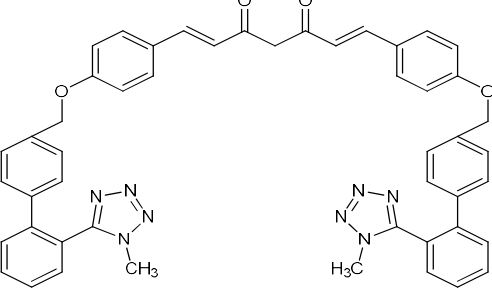
The basic nucleus of curcumin was subjected to structural modifications by retaining the alpha-beta diketone moiety to design fifteen analogues and sketched using the 2D sketcher of the Maestro tool in Schrodinger software (Table-1). The 2D structures were preprocessed, which checked the ionization conditions at neutral pH. The 2D structures were then changed into 3D structures (ligands) using the Lig-Prep tool of the Schrodinger software. The addition of hydrogen atoms, neutralizing charged groups, and optimizing the geometry of ligands was done using the Etk software.^{14,15}

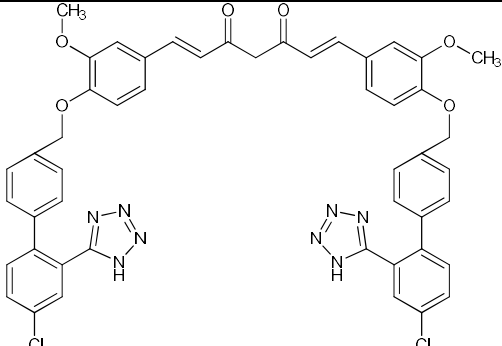
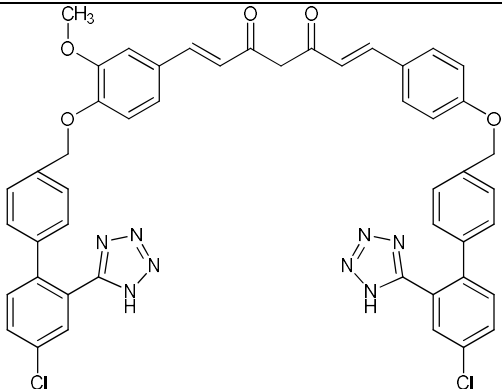
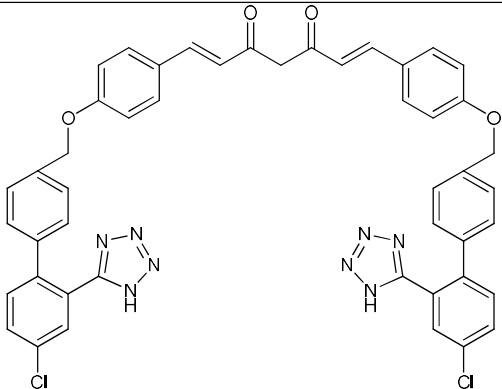
Table-1: Structures of Newly Designed Curcumin Analogues

Structure No.	Structures
---------------	------------

CA-1	 <p>(1E,6E)-1-[3-methoxy-4-(2'-[2-(triphenylmethyl)-2H-1,2,3,4-tetrazol-5-yl]-[1,1'-biphenyl]-4-yl)methoxy)phenyl]-7-[3-methoxy-4-(2'-[2-(triphenylmethyl)-2H-1,2,3,4-tetrazol-5-yl]-[1,1'-biphenyl]-4-yl)oxy)phenyl]hepta-1,6-diene-3,5-dione</p>
CA-2	 <p>(1E,6E)-1-[3-methoxy-4-(2'-[2-(triphenylmethyl)-2H-1,2,3,4-tetrazol-5-yl]-[1,1'-biphenyl]-4-yl)methoxy)phenyl]-7-(4-{2'-(2H-1,2,3,4-tetrazol-5-yl)-[1,1'-biphenyl]-4-yl}oxy)phenyl]hepta-1,6-diene-3,5-dione</p>
CA-3	 <p>(1E,6E)-1-(4-{[2'-(2H-1,2,3,4-tetrazol-5-yl)-[1,1'-biphenyl]-4-yl]oxy}phenyl)-7-[4-(2'-[2-(triphenylmethyl)-2H-1,2,3,4-tetrazol-5-yl]-[1,1'-biphenyl]-4-yl)methoxy)phenyl]hepta-1,6-diene-3,5-dione</p>
CA-4	 <p>(1E,6E)-1-[3-methoxy-4-(2'-[2-(triphenylmethyl)-2H-1,2,3,4-tetrazol-5-yl]-[1,1'-biphenyl]-4-yl)methoxy)phenyl]-7-(3-methoxy-4-{2'-(2H-1,2,3,4-tetrazol-5-yl)-[1,1'-biphenyl]-4-yl}oxy)phenyl]hepta-1,6-diene-3,5-dione</p>

CA-5	 <p>(1E,6E)-1-[3-methoxy-4-({2'-[2-(triphenylmethyl)-2H-1,2,3,4-tetrazol-5-yl]-[1,1'-biphenyl]-4-yl}methoxy)phenyl]-7-(4-{[2'-(2H-1,2,3,4-tetrazol-5-yl)-[1,1'-biphenyl]-4-yl]oxy}phenyl)hepta-1,6-diene-3,5-dione</p>
CA-6	 <p>(1E,6E)-1-(4-{[2'-(2H-1,2,3,4-tetrazol-5-yl)-[1,1'-biphenyl]-4-yl]oxy}phenyl)-7-[4-({2'-[2-(triphenylmethyl)-2H-1,2,3,4-tetrazol-5-yl]-[1,1'-biphenyl]-4-yl}methoxy)phenyl]hepta-1,6-diene-3,5-dione</p>
CA-7	 <p>(1E,6E)-1-(3-methoxy-4-{[2'-(2H-1,2,3,4-tetrazol-5-yl)-[1,1'-biphenyl]-4-yl]methoxy}phenyl)-7-(3-methoxy-4-{[2'-(2H-1,2,3,4-tetrazol-5-yl)-[1,1'-biphenyl]-4-yl]oxy}phenyl)hepta-1,6-diene-3,5-dione</p>
CA-8	 <p>(1E,6E)-1-(3-methoxy-4-{[2'-(2H-1,2,3,4-tetrazol-5-yl)-[1,1'-biphenyl]-4-yl]methoxy}phenyl)-7-(4-{[2'-(2H-1,2,3,4-tetrazol-5-yl)-[1,1'-biphenyl]-4-yl]oxy}phenyl)hepta-1,6-diene-3,5-dione</p>

CA-9	 <p>(1E,6E)-1-(4-{[2'-(2H-1,2,3,4-tetrazol-5-yl)-[1,1'-biphenyl]-4-yl]methoxy}phenyl)-7-(4-{[2'-(2H-1,2,3,4-tetrazol-5-yl)-[1,1'-biphenyl]-4-yl]oxy}phenyl)hepta-1,6-diene-3,5-dione</p>
CA-10	 <p>(1E,6E)-1,7-bis(3-methoxy-4-((2'-(1-methyl-1H-tetrazol-5-yl)-[1,1'-biphenyl]-4-yl)methoxy)phenyl)hepta-1,6-diene-3,5-dione</p>
CA-11	 <p>(1E,6E)-1-(3-methoxy-4-((2'-(1-methyl-1H-tetrazol-5-yl)-[1,1'-biphenyl]-4-yl)methoxy)phenyl)-7-(4-((2'-(1-methyl-1H-tetrazol-5-yl)-[1,1'-biphenyl]-4-yl)methoxy)phenyl)hepta-1,6-diene-3,5-dione</p>
CA-12	 <p>(1E,6E)-1,7-bis(4-((2'-(1-methyl-1H-tetrazol-5-yl)-[1,1'-biphenyl]-4-yl)methoxy)phenyl)hepta-1,6-diene-3,5-dione</p>

CA-13	 <p>(1E,6E)-1,7-bis(4-((4'-chloro-2'-(1H-tetrazol-5-yl)-[1,1'-biphenyl]-4-yl)methoxy)-3-methoxyphenyl)hepta-1,6-diene-3,5-dione</p>
CA-14	 <p>(1E,6E)-1-(4-((4'-chloro-2'-(1H-tetrazol-5-yl)-[1,1'-biphenyl]-4-yl)methoxy)-3-methoxyphenyl)-7-(4-((4'-chloro-2'-(1H-tetrazol-5-yl)-[1,1'-biphenyl]-4-yl)methoxy)phenyl)hepta-1,6-diene-3,5-dione</p>
CA-15	 <p>(1E,6E)-1,7-bis(4-((4'-chloro-2'-(1H-tetrazol-5-yl)-[1,1'-biphenyl]-4-yl)methoxy)phenyl)hepta-1,6-diene-3,5-dione</p>

Protein Selection, Preparation, and Validation

From the protein data bank, the KRAS protein was selected and imported to the workplace (Fig.-2). To obtain a clear picture, proteins from Homo sapiens with a resolution of 1.35 Å were chosen.¹⁶ The target protein, GTPase KRAS, has a sequence length of 170 amino acids that includes both polar and non-polar amino acids. Selected proteins were prepared for docking purposes using the "Protein Preparation Wizard" workflow in the Schrodinger suites.^{15,17,18} The preprocessed ligand was prepared for docking using Ligprep from the Schrodinger suite. Target proteins were then docked using SP mode via Glide of the Schrodinger suite's Maestro tool. To calculate the RMSD value, the target was superimposed on the

preprocessed ligand, and the target was computed. The value obtained was $1.289 \text{ \AA} \approx 1.290 \text{ \AA}$. The superimposition of the docked ligand on the pre-processed ligand validates that the designed molecules can be docked with the target.¹⁵

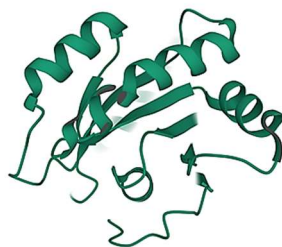


Fig.-2: X-Ray Crystallographic Structure of Protein 4EPV

Receptor Grid Generation

The grid was created by using Schrodinger Software 2016's Receptor Grid Generation tool to identify the binding pocket where the molecule would bind with the target.¹⁵

Glide Ligand Docking

Prepared ligands and proteins were docked with standard precision using the Glide (grid-based ligand docking with energetics) algorithm in the Standard Precision (SP) mode. An Optimized Potentials for Liquid Simulations (OPLS) force field was used for all the calculations. Glide docking tests were performed on Linux systems.^{15,17,19} Docking of gemcitabine, dabrafenib, and curcuminoids was done with the same target to compare the docking results with fifteen designed novel molecules.²⁰⁻²⁴

Docking Studies

The docking analysis was performed in the Schrodinger software 2016 Maestro using the Glide tool. With rigid ligands, prepared ligands were docked into the active site of the target protein KRAS. Docking analysis was first carried out on the co-crystallized ligand to determine its binding affinity at the active site of the target protein prior to docking. To view the interaction image of the ligands with the residues at the active site of the KRAS protein, the ligand interaction tool was used.

ADMET Studies

The antagonistic behaviour of an inhibitor of a protein or an enzyme does not give any assurance of the suitability of a drug candidate as an imminent drug. Furthermore, these clinical trials of medications with inadequate ADME studies cause irreparable damage to the biological systems due to an excess of toxicity. Hence, analysis for ADME (absorption, distribution, metabolism, and excretion) and drug-likeness becomes critical during drug discovery.^{25,26} ADMET properties of the hit molecules identified by docking studies were conducted and results were compiled and compared to get a better idea of the drug's behaviour inside the body. By using SMILES (Simplified Molecular Input Line Entry System), all three curcumin analogues were imported into the above-mentioned programmes to generate a pharmacokinetic profile or drug-likeness specification.²⁷ In order to check the safety profile and oral activeness (drug-likeness) of medicine in the human body, in 1997, a thumb rule was developed by Christopher A. Lipinski, i.e., Lipinski's rule of five, or Pfizer's rule of five. If the drug data corresponded to the given cutoff values, then there was no violation of Lipinski's Rule.²⁸

Isolation of Curcuminoids

According to Scheme-1, 5 g of turmeric was subjected to column chromatography to isolate the curcuminoids using silica gel as the stationary phase and benzene/ethyl acetate as the eluent. Eluent fractions 82:18 separated out curcumin (74%), 70:30 separated out demethoxy curcumin (70%), and 54:48 separated out bisdemethoxycurcumin (60%).

Synthesis of CA-7, CA-8, and CA-9 Molecules

Equimolar amounts of isolated curcuminoids and bromobiphenyl triphenyl tetrazole were mixed and refluxed for 10-12 hours, with thin layer chromatography (TLC) checking intermittently. The reaction

mixture was then filtered through Hyflow layers using suction. The solid was then separated from the Hyflow using methanol and purified by recrystallization (Scheme-1a, b, and c) (Fig.-3).

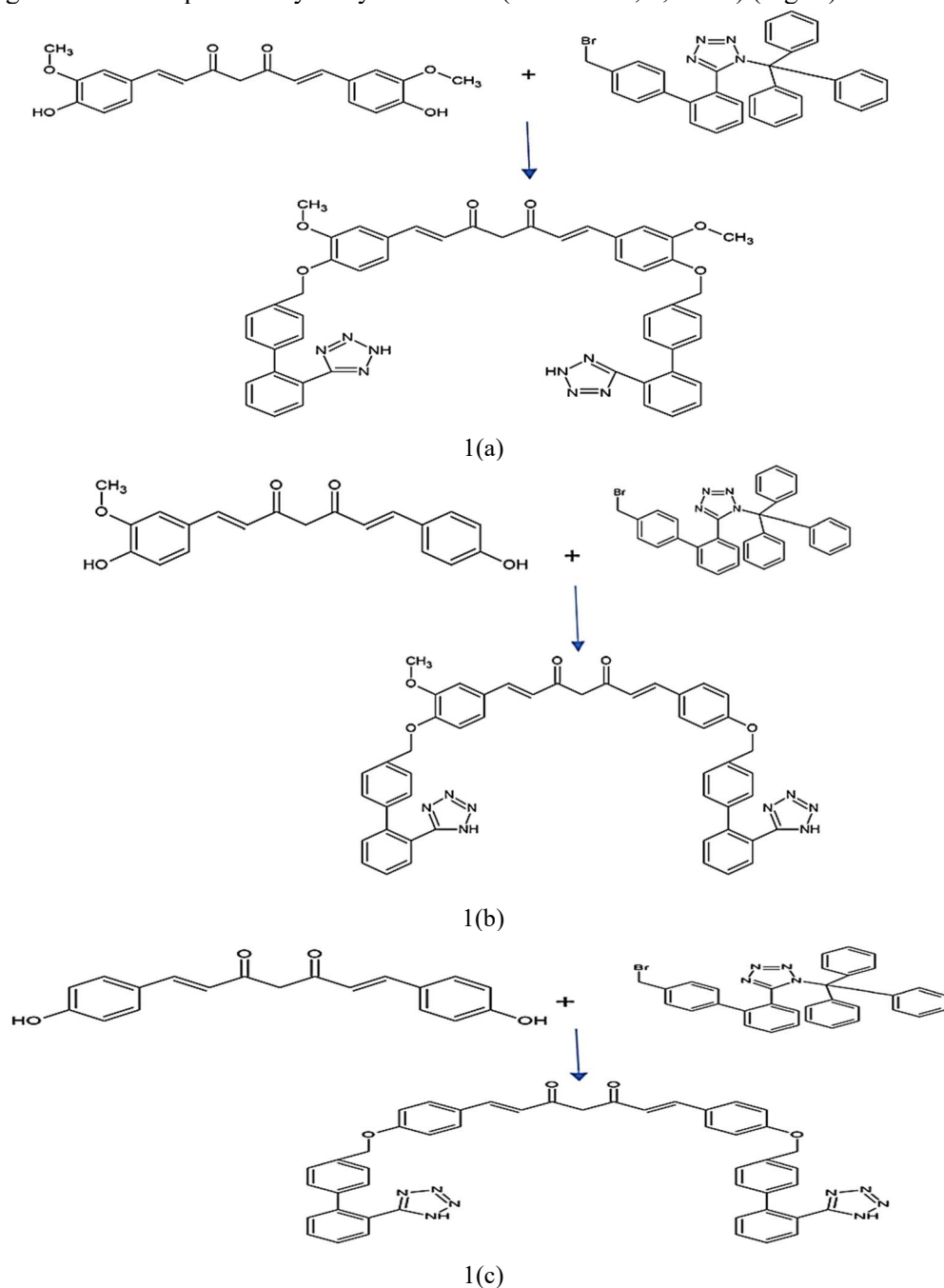


Fig.-3: Scheme 1 - Schematic Plan for Synthesis of (1a) CA-7, (1b) CA-8 and (1c) CA-9

Characterization and Stability

For structural determination, synthetic curcumin analogues were subjected to NMR, IR, and mass spectrographic analysis.²⁹ To conduct the stability test, a 0.1g sample was used. A stability test was carried out under the headings of acid hydrolysis, base hydrolysis, thermal degradation, and photolytic degradation for 24 h, 1 month, and 3 months as per the standard procedure using a UV-VIS spectrophotometer.³⁰

Anticancer Activity by MTT Assay

The cytotoxicity of all three synthesised curcumin analogues was evaluated using a 3-(4, 5-dimethylthiazol-2-yl)-2, 5-diphenyltetrazolium bromide assay (MTT assay).³¹ The cells were seeded overnight in a

microplate of 96-well flat-bottom by maintaining 37 °C temperature with 5% CO₂ and 95% humidity. Different concentrations (100, 50, 25, 12.5, 6.25, and 3.125 µg/ml) of samples were treated, and all cells were further incubated for the next 48 h. After washing the wells twice with phosphate-buffered saline solution (PBS), 20 µl of the MTT solution was added to each well, and the plates were incubated at 37 °C. After 4 h, to dissolve the formazan crystals, 100 µl of dimethyl sulfoxide (DMSO) was added to each well, and absorbance was logged at 570 nm using a microplate reader. As a control, doxorubicin was used to compare the potency of each curcumin analogue. The absorbance of the culture medium without PANC-1 cell lines was taken as blank and subtracted. The vehicle control was the PANC-1 cell lines which were treated with a suitable concentration of DMSO. By using Graph Pad Prism Version 5.1 software, the IC₅₀ values (50% inhibition concentration of the drug molecule) of novel drug molecules were calculated. The percentage of cell viability was calculated for each concentration by dividing the sample OD by the control OD, i.e.

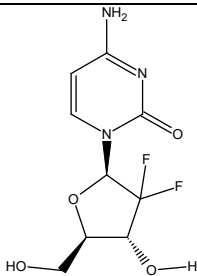
Surviving cells (%) = Mean OD of test compound / Mean OD of negative control x 100.

RESULTS AND DISCUSSION

Molecular Docking Study

One common feature of the two drugs, Gemcitabine and Dabrafenib, is that both have a pyrimidine ring and an amino group. In both gemcitabine and dabrafenib, an amino group is present on the pyrimidine ring.³² On studying the 2D structure of ligand interaction with the target, it has been observed that hydroxyl groups are present both outwards and inwards on the furan ring. One hydroxyl group attached to the furan ring shows backbone hydrogen bond interaction with two amino acids, Asp54 with a bond length of 2.24 Å and Leu 6 with a bond length of 1.93 Å. The other hydroxyl group shows sidechain bond interaction with Asp54 which has a bond length of 2.22 Å. Docking scores of the newly designed derivatives showed interactions with the target protein. In the ligand interaction, images of the docked curcumin analogues' π -cation interaction are observed in most of the derivatives. This claims the ability of newly designed curcumin analogues to bind inside the pocket of the target protein. Designed derivatives showed π -cation interaction with Lysine117, Lysine147 and backbone H-bond or, in some cases, salt bridges with Serine 17, Serine 39, Alanine 18, Aspartic acid 54, Glutamine 70, Threonine and Tyrosine 71.^{33,34} The docking results are tabulated in Table-2 and Table-3. Demethoxy curcumin, has the strongest binding affinity, with a docking score of -3.931, which is higher than the parent compounds. 2D and 3D frames show π -cation interaction with Arginine 154 having a bond length of 6.43 Å and backbone hydrogen interaction with Glycine 70 having a bond length of 2.54 Å. Results of Table-3 suggest that among all 15 newly designed curcumin analogues, three-CA-7, CA-8, and CA-9 displayed better docking scores compared to their parent compounds and other designed analogues. Thus, these three were identified as hit molecules. CA-1 and CA-2 exhibited nil docking scores which reveal their inability to fit into the pocket of the target.

Table-2: Docking Score and Glide Energy of Commercially Available Anti-Cancer Drugs and Parent Molecules

Parent Compound	Docking Score	Glide Energy (kcal/mol)	H-Bond	Bond length Å°
 Gemcitabine	-3.8	-32.428	Asp54 backbone	2.22
			Leu6 backbone	1.93

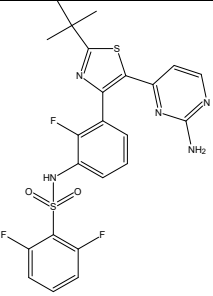
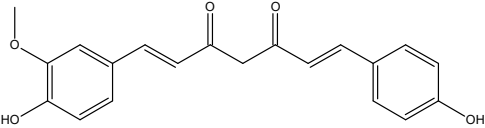
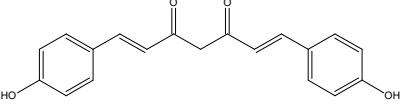
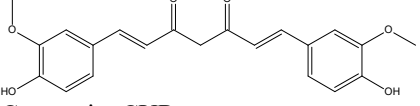
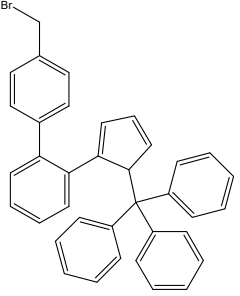
 <p>Dabrafenib</p>	-3.546	-41.748	Glu62 (SideChain)	1.68
 <p>Demethoxy Curcumin (DMCUR)</p>	-3.931	-49.367	Arginine154 Π -cation Glycine70 Backbone	6.43 2.54
 <p>Bis Demethoxy Curcumin BDMCUR</p>	-3.263	-39.344	Methonine 69- Halogen bond	3.23
 <p>Curcumin, CUR</p>	-3.876	-51.006	Leucine backbone 6 Aspartine 38 backbone	1.98 1.94
 <p>Bromobiphenyl Triphenyl Tetrazole (BBTT)</p>	-3.717	-45.354	Glutamine70 Backbone Leucine6 Halogen bond	2.31 3.35

Table-3: Docking Score and Glide Energy of Newly Designed Curcumin Analogues

Curcumin Derivatives	Docking Score	Glide Energy(kcal/mol)
CA-8	-6.810	-70.305
CA-9	-6.445	-56.404
CA-7	-6.110	-49.773
CA-9 (conformer)	-3.054	-53.409
CA-8 (conformer)	-2.875	-34.578
CA-15	-3.763	-49.76
CA-14	-3.758	-49.10
CA-6	-3.745	-48.50
CA-5	-3.741	-47.01
CA-4	-3.694	-42.22
CA-12	-3.646	-52.24
CA -11	-3.431	-47.04
CA-10	-3.390	- 47.03
CA-13	-3.281	-45.36
CA-3	-3.097	-36.46

Binding Poses of CA-7

The docking score of CA-7 is -6.110, and the glide energy is -49.773 kcal/mol. The phenyl ring attached to the tetrazole moiety shows π -cation binding with Lysine 117 having a bond length of 4.41 Å (Fig.-4). With a bond length of 6.23 Å, the tetrazole moiety also exhibits π -cation binding with Lysine 147. The nitrogen of the tetrazole moiety shows a backbone hydrogen bond, with Serine 17 and Alanine 18 having a bond length of 2.39 Å and 2.52 Å respectively. CA-7 has higher gliding energy (-49.773 kcal/mol) than the standard drugs gemcitabine (-32.428) and dabrafenib (-41.748), indicating that the designed compound's binding ability with the target is comparable.³⁵

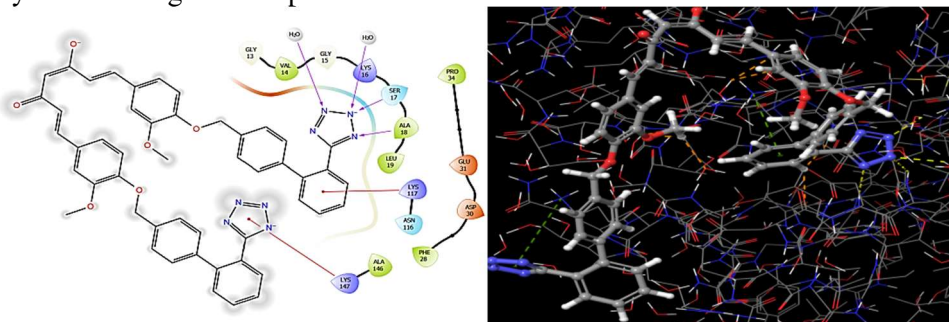


Fig.-4: Molecular Docking Model of CA-7 with 4EPV (a) 2D Interaction Map for Docking of CA- 7 with 4EPV and (b) 3D Model

Binding Poses of CA-8

The phenyl ring attached to the tetrazole moiety of CA-8 exhibited π -cation binding with Lysine 117, with a bond length of 4.60 Å (Fig.-5). The nitrogen of the tetrazole moiety shows a backbone hydrogen bond with Serine 17 and Alanine 18, having a bond length of 2.31 Å and 2.58 Å respectively. On comparing the glide energy of CA-8 with that of standard drugs gemcitabine and dabrafenib, it is evident that the glide energy of novel molecule CA-8 is much better, which confirms the tight binding of the designed molecule with the target. Another conformer of the same derivative (CA-8) showed varied binding with the target (Fig.-6). This conformer has a backbone hydrogen bond with Serine 17 (2.38) and Alanine 18 (2.25), but it also has a salt bridge with Lysine 147 (4.25) and a π -cation bond (3.68). It also demonstrates a π -cation bond with Lysine 117 (4.57).³⁶

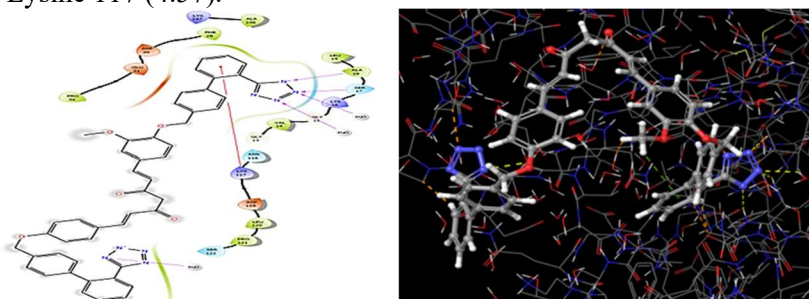


Fig.-5: Molecular Docking Model of CA-8 with 4EPV (a) 2D Interaction Map for Docking of CA- 8 with 4EPV and (b) 3D Model

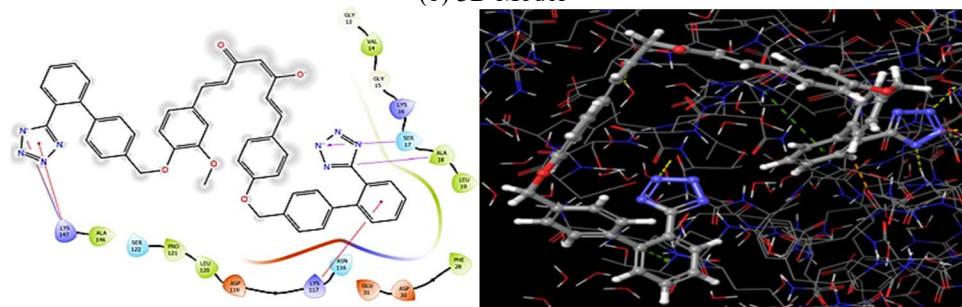


Fig.-6: Molecular Docking Model of CA-8 Conformer with 4EPV (a) 2D Interaction Map for Docking of CA- 8 with 4EPV and (b) 3D model

The phenyl ring attached to the tetrazole moiety of CA-9 shows π -cation binding with Lysine 117 (4.41) (Fig.-7). The nitrogen of the tetrazole moiety shows a backbone hydrogen bond with Serine 17 and Alanine 18, with bond lengths of 2.37 and 2.50, respectively. CA-9 has lower gliding energy (-56.404 kcal/mol) than gemcitabine (-32.428) and dabrafenib (-41.748), indicating a strong binding with the target protein.³⁷ Another conformer of CA-9 has a docking score of -3.054 and a glide energy of -53.409 kcal/mol (Fig.-8). This conformer shows a backbone hydrogen bond with Serine 17 and Alanine 18, having bond lengths of 2.30 Å and 2.60 Å respectively, along with two π -cation interactions with bond lengths of 5.99 Å and 4.57 Å.³⁸

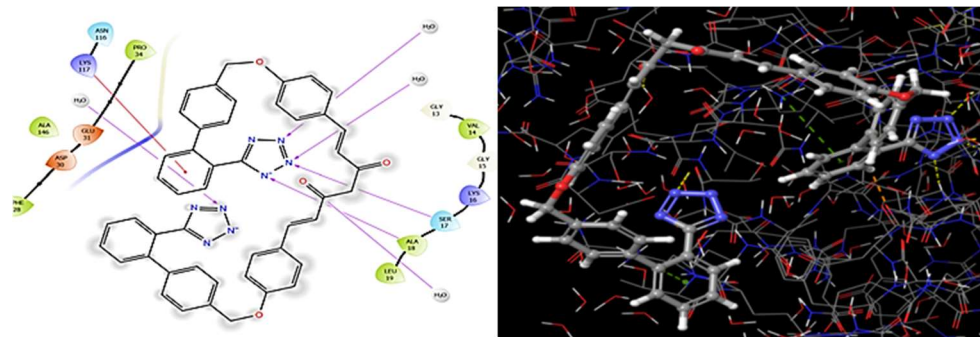


Fig-7: Molecular Docking Model of CA-9 with 4EPV (a) 2D Interaction Map for Docking of CA- 9 with 4EPV and (b) 3D model

The physicochemical properties such as molecular weight, lipophilicity, topological polar surface area, acceptors, and donors of hydrogen bonds and drug-likeness of CA-7, CA-8, and CA-9 are presented in Table-4. They satisfy Lipinski's Rules of three and five. The ADMET properties of the synthesized compounds are shown in Table-5. These novel molecules are inhibitors of cytochrome 450 enzymes and are poorly distributed to the brain, thus, they are not capable to pass through the BBB (Blood-brain barrier). They have a low clearance rate, and shorter half-life. Out of the three molecules, only CA-9 is mutagenic.

Parameters	Standard value	CA-7	CA-8	CA-9
MW (Molecular weight)	<500	822.87 g/mol	792.84 g/mol	762.81 g/mol
MLogP (Moriguchi octanol-water partition coefficient)	≤4.15	5.01	5.33	5.65
nHBA (number of H-bond acceptor)	≤10	12	11	10
nHBD (number of H-bond donor)	≤5	2	2	2
Lipinski's Rule	Yes; 0 or 1 violation	No; 3 violations: MW>500, MLOGP>4.15, nHBA > 10	No; 3 violations: MW>500, MLOGP>4.15, nHBA > 10	No; 3 violations: MW>500, MLOGP>4.15, nHBA > 10
WLOGP (Lipophilicity; n-octanol / water partition coefficient)	≤5.88	8.65	8.65	8.64
TPSA (Topological Polar Surface Area)	≤131.6 Å ²	179.98 Å ²	170.75 Å ²	161.52 Å ²
Egan's Rule	Yes; 0 violation	No; 2 violations: WLOGP>5.88, TPSA>131.6	No; 2 violations: WLOGP>5.88, TPSA>131.6	No; 2 violations: WLOGP>5.88, TPSA>131.6
Bioavailability Score	0.55	0.11	0.11	0.11

Synthesis

Table-5: ADMET Studies of CA-7, CA-8 and CA-9

Parameters	Standard value	CA-7	CA-8	CA-9
Adsorption				
Caco-2 Permeability	Optimal condition: higher than -5.15 Log unit	-5.478	-5.461	-5.444
Pgp (P-glycoprotein) substrate	Yes – substrate; No - non-substrate	Yes	Yes	No
Pgp (P-glycoprotein) I inhibitor	Yes – substrate; No - non-substrate	Yes	Yes	No
Pgp (P-glycoprotein) II inhibitor	Yes – substrate; No - non-substrate	Yes	Yes	Yes
Distribution				
BBB (Blood Brain Barrier) Permeability (log BB)	Log BB > 0.3 (high); Log BB < -1 (poor)	-3.392 (BBB-)	-3.229 (BBB-)	-3.036 (BBB-)
CNS (Central Nervous System) Permeability (log PS)	Log PS > -2 (penetrate); Log PS < -3 (difficult to penetrate)	-4.095	-3.817	-3.679
VDss (Volume of Distribution); human	Log VDss > 0.45 (high); Log VDss < -0.15 (low)	-0.264	-0.188	-0.286
Metabolism				
CYP1A2 enzyme	Yes – inhibitor; No - non-inhibitor	No	No	No
CYP2C19 enzyme	Yes – inhibitor; No - non-inhibitor	No	Yes	Yes
CYP2C9 enzyme	Yes – inhibitor; No - non-inhibitor	No	No	Yes
CYP2D6 enzyme	Yes – inhibitor; No - non-inhibitor	No	No	No
CYP3A4 enzyme	Yes – inhibitor; No - non-inhibitor	Yes	Yes	Yes
Excretion				
CL	High: >15 mL/min/Kg; moderate: 5-15 mL/min/Kg; low: <5 mL/min/Kg	1.025	0.606	0.365
T _{1/2}	1: long half-life; 0: short half-life	0.016	0.009	0.005
Toxicity				
Hepatotoxicity	Yes – inhibitor; No - non-inhibitor	Yes	Yes	Yes
hERG (human ether-a-go-go-related gene) I inhibitor	Yes – inhibitor; No - non-inhibitor	No	No	No
hERG (human ether-a-go-go-related gene) II inhibitor	Yes – inhibitor; No - non-inhibitor	Yes	Yes	Yes
Ames Test	0-0.3: excellent; 0.3-0.7: medium; 0.7-1.0: poor	Negative 0.823	Negative 0.727	Positive 0.614

For the synthesis of curcumin analogues with a tetrazole moiety, the reaction was carried out in two sets. In the first set of reactions, the first curcuminoids (curcumin, demethoxy curcumin, and bisdemethoxy curcumin) were isolated by column chromatography, and then the reaction continued. The yield of the

curcumin analogues CA-7 to CA-9 was sufficient for further investigation. The percentage yield of curcumin analogue, demethoxy curcumin analogue, and demethoxy curcumin analogue was about 74% w/w, 70% w/w, and 60% w/w, respectively.³⁹

Characterization

CA-7

¹H NMR of CA-7 in DMSO δ -3.8 (s 6H, OCH₃ of Curcumin), δ -4.4 (2H methylene between diketo group), δ =6.7 to δ =7.6 (aromatic H). δ (ppm): 7.69 (d, J = 7.2 Hz, 2H), 7.68 (t, J = 3.6 Hz, 1H), 7.53 – 7.58 (m, 3H), 7.39 (d, J = 7.6 Hz, 1H), 7.30 – 7.37 (m, 2H) [Curcumin 6.06 (s, 1H), 6.73 (d, 2H), 7.56 (d, 2H), 7.32, 6.83, 7.16, 3.83 (s, 3H)]. The peaks in the range of 1261 cm⁻¹ to 1214 cm⁻¹ confirm the ether linkage in a molecule.⁴⁰ Peaks at 1618 and 1608 cm⁻¹ indicate the presence of α , β diketo group. The peak at 1906 cm⁻¹ shows the presence of a benzene nucleus. Peaks at 1109 cm⁻¹ and 1134 cm⁻¹ are corresponds to tetrazole ring.⁴¹ The remaining peaks confirm aromatic rings. Peaks in the province of 1975 cm⁻¹ to 1615 cm⁻¹ agree with the presence of combined aromatic bands. Calculated LC/MS (*m/z*): 836.89, and graphical LC/MS (*m/z*): 837.53.

CA-8

¹H NMR of CA -8 in DMSO δ -3.8. δ -3.8 (s 3H, OCH₃ of Curcumin) δ -4.4 (2H methylene between diketo group), δ =6.7 to δ =7.6 (aromatic H). δ -4.4 (2H methylene between α , β diketo group), δ =6.7 to δ =7.6 (aromatic H). δ (ppm): 7.69 (d, J = 7.2 Hz, 2H), 7.68 (t, J = 3.6 Hz, 1H), 7.52 – 7.58 (m, 3H), 7.39 (d, J = 7.6 Hz, 1H), 7.31 – 7.39 (m, 2H) [Curcumin 6.06 (s, 1H), 6.73 (d, 2H), 7.56 (d, 2H), 7.32, 6.83, 7.16, 3.83 (s, 3H)]. Distinct peaks in the range of 1261 cm⁻¹ to 1214 cm⁻¹ confirm the ether linkage in the molecule.⁴⁰ The presence of α , β diketo group is indicated by sharp peaks at 1618 and 1608 cm⁻¹. The peak at 1906 cm⁻¹ approves the presence of a benzene nucleus. Peaks at 1109 cm⁻¹ and 1134 cm⁻¹ correspond to tetrazole ring.⁴¹ There were fewer peaks in the region of 2955 cm⁻¹ to 2853 cm⁻¹ when compared to the graphs of curcumin analogues, which confirms the absence of one -OCH₃ group⁴² and the remaining peaks confirm aromatic rings. Peaks at 1975 cm⁻¹ to 1615 cm⁻¹ specify the presence of combined aromatic bands. On comparing the calculated mass (806.87 *m/z*) of CA-8 with LC-MS, it is found to be 807.57 *m/z* which is closer to the calculated one.

CA-9

In ¹H NMR of CA-9, the peak at δ -3.8Hz is absent which confirms the absence of OCH₃ in this derivative, δ -4.4 (2H methylene between diketo group), δ =6.7 to δ =7.6 (aromatic H), δ (ppm): 7.65 (d, J = 7.2 Hz, 2H), 7.66 (t, J = 3.6 Hz, 1H), 7.52 – 7.59 (m, 3H), 7.32 (d, J = 7.6 Hz, 1H), 7.52 – 7.59 (m, 2H) [Curcumin 6.06 (s, 1H), 6.73 (d, 2H), 7.56 (d, 2H), 7.32, 6.83, 7.16, 3.84 (s, 3H)]. The peaks in the array of 1261 cm⁻¹ to 1214 cm⁻¹ confirm the ether linkage in a molecule.⁴⁰ The presence of α , β diketo group is indicated by the presence of peaks at 1618 and 1608 cm⁻¹. The distinct peak at 1906 cm⁻¹ expresses the presence of a benzene nucleus. Peaks at 1109 cm⁻¹ and 1134 cm⁻¹ are correspond to the tetrazole ring.⁴¹ The number of peaks in 2955 cm⁻¹ to 2853 cm⁻¹ region is less when compared to the graphs of curcumin analogue and demethoxy curcumin analogues, this confirms the absence of the -OCH₃ group.⁴² Distinct peaks appearing from 1975 cm⁻¹ to 1615 cm⁻¹ specify the presence of combined aromatic bands. The calculated mass (776.84 *m/z*) and observed LC/MS (777.44 *m/z*) are quite close.⁴³

Stability

Stability tests for all three molecules (CA-7, CA-8, and CA-9) were done by the UV-VIS spectrophotometer, and the results are shown in Fig.-9 to 11. It was found that CA-7 and CA-9 were stable for a period of 24 h and a period of 1 month, while after a period of three months, slight degradation was seen (Fig.-9a-d and 11a-d). From Fig.-10a-d of CA-8, it is apparent that no changes were seen within the tested period. Thus, it can be assumed that the compound is stable in the given conditions but requires further confirmation.

Stability results for CA-7

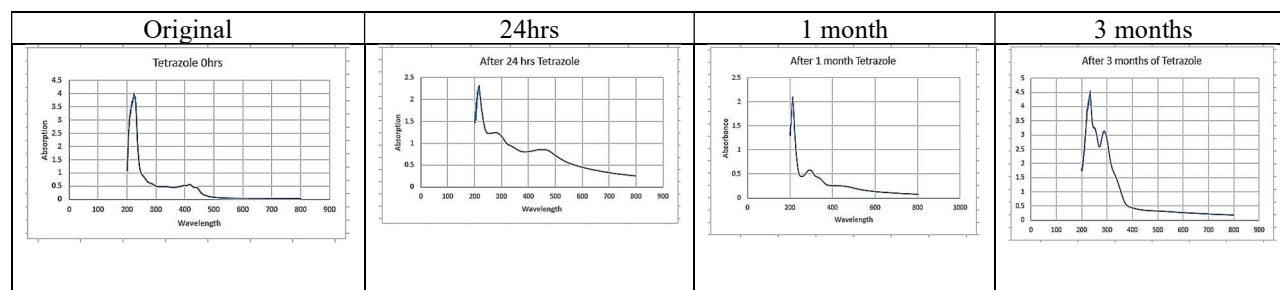


Fig.-9(a): Acid hydrolysis of CA-7

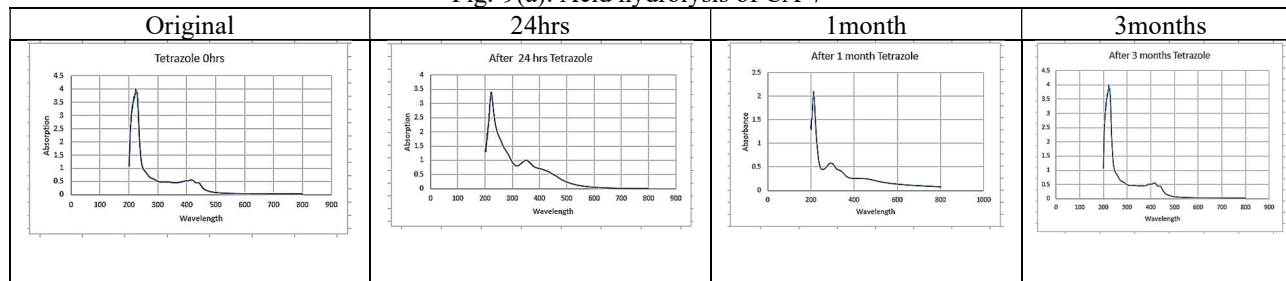


Fig.-9(b): Base hydrolysis of CA-7

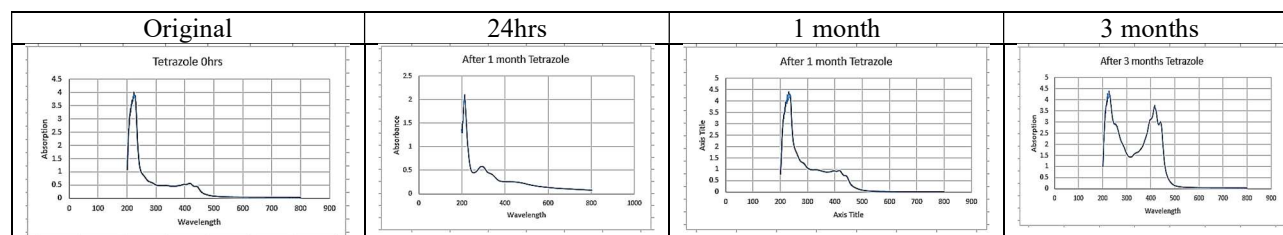


Fig.-9(c): Thermal degradation of CA-7

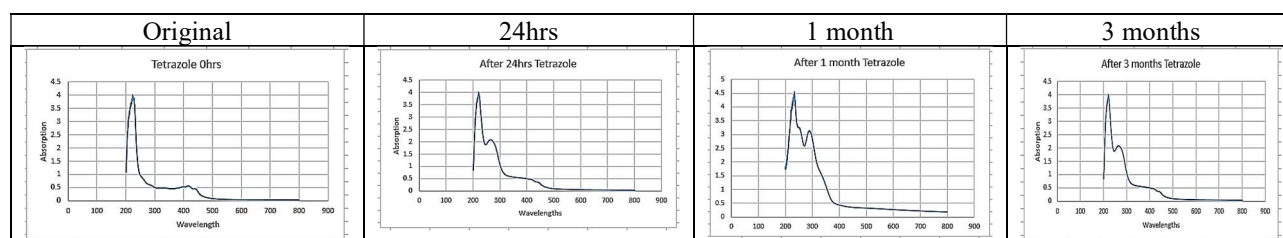


Fig.-9(d): Photolytic degradation of CA-7

Stability results for CA-8

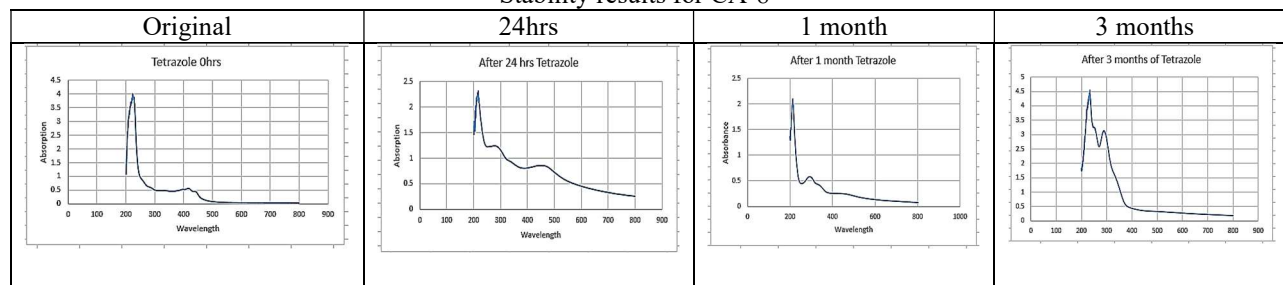


Fig.-10(a): Acid hydrolysis of CA-8

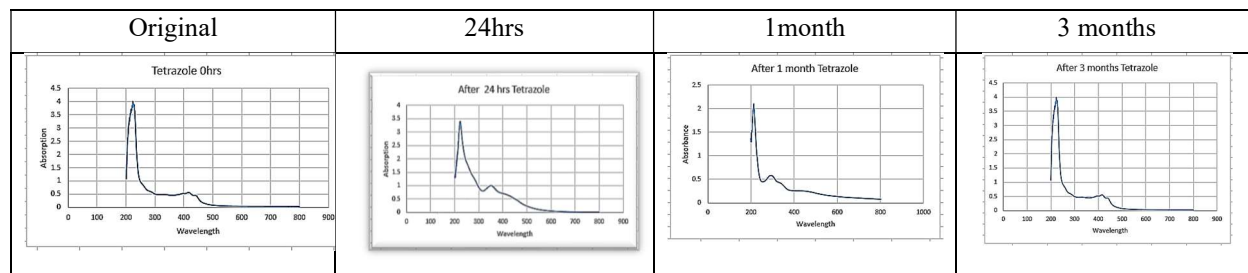


Fig.-10(b): Base Hydrolysis of CA-8

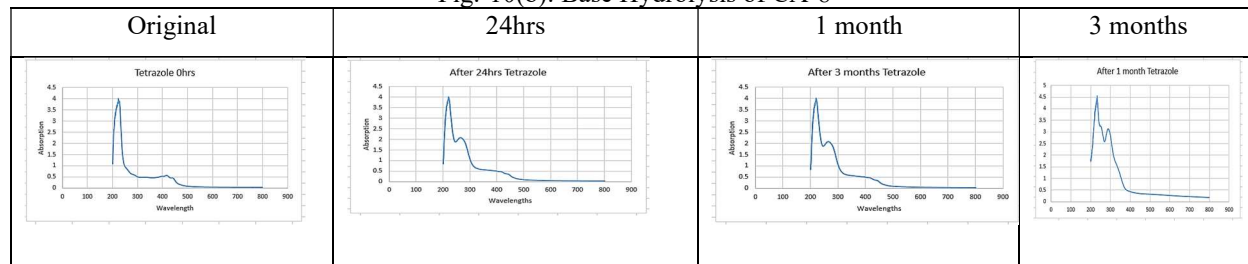


Fig.-10(c): Thermal Degradation of CA-8

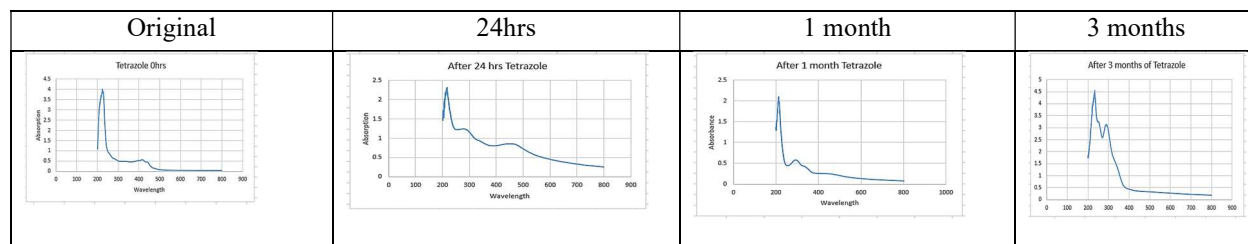


Fig.-10(d): Photolytic Degradation of CA-8

Stability Results for CA-9

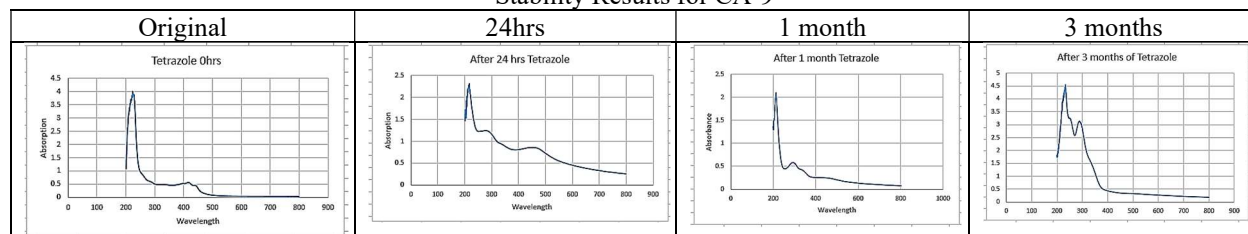


Fig.-11(a): Acid Hydrolysis of CA-9

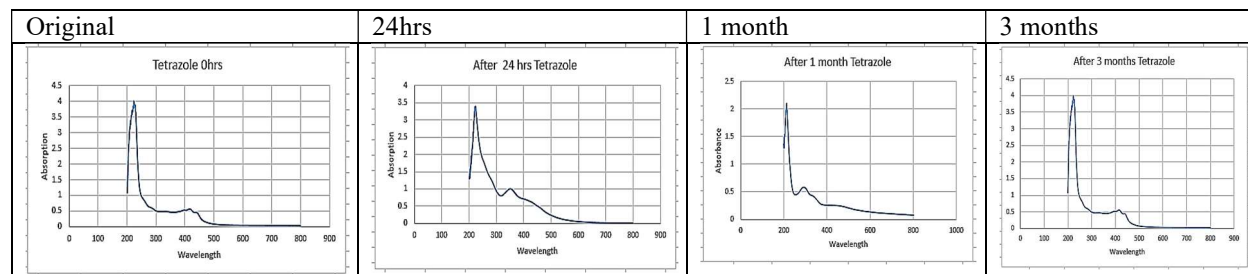


Fig.-11(b): Base Hydrolysis of CA-9

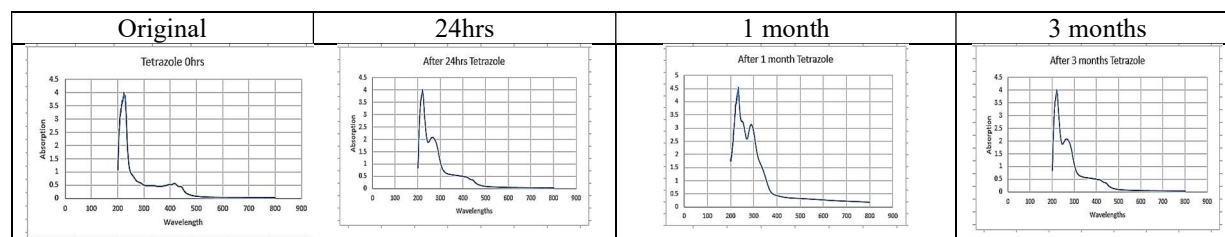


Fig.-11(c): Thermal Degradation of CA-9

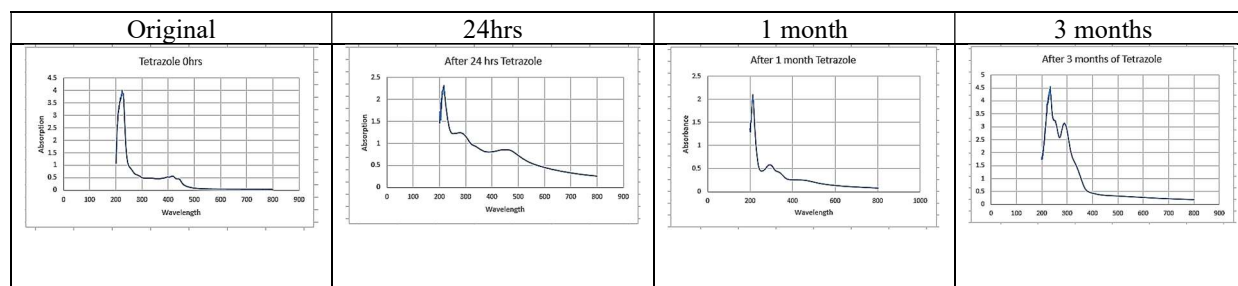


Fig.-11(d): Photolytic Degradation of CA-9

Anticancer Activity by MTT Assay

The ant proliferative activity of CA-7, CA-8, and CA-9 was evaluated by the MTT assay on PANC-1 cell lines. Results were compared with the positive control, doxorubicin. The IC₅₀ values of all three curcumin analogues are 82.2 $\mu\text{g/ml}$, 153.73 $\mu\text{g/ml}$ and 204.60 $\mu\text{g/ml}$ for CA-9, CA-8 and CA-7 respectively (Fig.-12). Calculated values of IC₅₀ are quite eloquent and suggest that CA-9 possesses better potency than the other derivatives. At the highest concentration (100 $\mu\text{g/ml}$) of CA-9, the cell viability percentage reduced to 34.61%, which is quite close to doxorubicin (26.8%), used as a positive control. This concludes that the synthesized curcumin analogues do inhibit the proliferation of cells and hence exhibit anticancer activity against PANC-1 cell lines. All the available data incline us to state that the synthesized curcumin analogues do inhibit the proliferation of cells. Still, there is a scope for structural modifications to enhance their anticancer efficacy against PANC-1 cell lines.

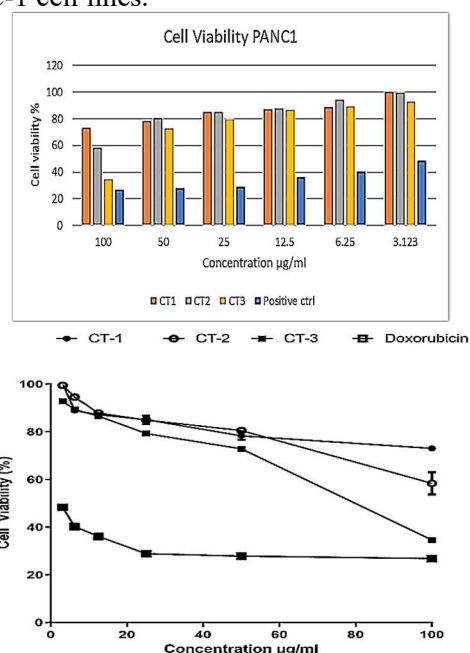


Fig.-12: Cell Viability % of CA-7, CA-8 and CA-9 Against PANC-1 Cell Lines (CT-1, CT-2 and CT-3 Represent CA-7, CA-8 and CA-9 Respectively)

CONCLUSION

The current study used pharmacophore-based designing and synthesis of hybrid compounds using phytochemicals to obtain a potential drug molecule as an anticancer agent against PANC-1 cell lines. For the first time, three new hybrid molecules (CA-7, CA-8, and CA-9) were synthesised using curcumin as a phytochemical and tetrazole as a pharmacophore, and their structures were confirmed by modern analytical techniques such as ¹HNMR, FTIR, and mass spectrometry. ADME studies suggest that all three synthesized drug molecules have CNS (Central Nervous System) and cell permeability. The available ADME data for novel curcumin analogues demonstrate their lipophilic nature with low bioavailability, implying poor oral adsorption and toxicity profiles, and indicating their suitability as a drug molecule. Stability studies confirm the stability of all three curcumin analogues in the given conditions, but slight changes were seen after a 3-month period, which requires further confirmation. *In vitro* antitumor activity was carried out by the MTT assay. Persuasive IC₅₀ values of CA-9 (82.2 µg/ml) and its positive Ames test conclude that among all three synthesized novel curcumin analogues, CA-9 is mutagenic and thus can be treated as a carcinogen. Results demonstrated that the curcumin-tetrazole conjugate exhibited substantial anticancer activity. Hence, the present study opens a new avenue to develop novel and superior anticancer drug molecules by performing different structural modifications in the base structure, which might lead to the discovery of more potent anticancer molecules against PANC-1 cell lines.

ACKNOWLEDGEMENTS

The reported work was partially funded by Karnataka Science and Technology Academy (KSTA), Department of Science and Technology, Government of Karnataka, India. The authors are thankful to M.S. Ramaiah University of Applied Sciences, Bangalore, India for giving us the opportunity to carry out this research work, including molecular docking studies, synthesis, and ADME studies, by providing the working space and requisite apparatus and chemicals.

CONFLICT OF INTERESTS

The authors declare no conflicts of interest.

AUTHOR CONTRIBUTIONS

All the authors contributed significantly to this manuscript, participated in reviewing/editing and approved the final draft for publication. The research profile of the authors can be verified from their ORCID ids, given below:

Lairikyengbam Deepti Roy  <https://orcid.org/0000-0002-2244-4345>

Jyotsna Kumar  <https://orcid.org/0000-0002-7138-4190>

Geeta Krishnamurthy  <https://orcid.org/0000-0001-9732-2038>

Pooja Gour  <https://orcid.org/0000-0002-3225-8263>

Shivanjali Esther Arland  <https://orcid.org/0000-0002-2591-180X>

Open Access: This article is distributed under the terms of the Creative Commons Attribution 4.0 International License (<http://creativecommons.org/licenses/by/4.0/>), which permits unrestricted use, distribution, and reproduction in any medium, provided you give appropriate credit to the original author(s) and the source, provide a link to the Creative Commons license, and indicate if changes were made.

REFERENCES

1. R. Siegel, K. Miller, H. Fuchs and A. Jemal, *Cancer Statistics*, **71(1)**, 7(2021), <https://doi.org/10.3322/caac.21654>
2. H. Momna, Introduction to Cancer Biology, 2nd Edition, Momna Hejmadi & Ventus Publishing ApS, p.6, (2010).
3. D. Hanahan and R. A. Weinberg, *Cell*, **100(1)**, 57(2011), <https://doi.org/10.1016/j.cell.2011.02.013>
4. J. M. Rhett, I. Khan and J. P. O'Bryan, *Advances in Cancer Research*, **148**, 69(2020), <https://doi.org/10.1016/bs.acr.2020.05.002>

5. P. Jason, P. Jason, C. B. Michael, T. Edward, A. Olejniczak, L. Taekyu, W. Olivia and W. F. Stephen, *Angewandte Chemie International Edition*, **51(25)**, 1(2012), <https://doi.org/10.1002/anie.201201358>
6. Z. Yan, L. Marie-Helene, M. Leila, A. Hemanth, M. Brown, and R. S. Brent, *Biochemistry*, **57(8)**, 1380(2018), <https://doi.org/10.1021/acs.biochem.7b01113>
7. S. Eser, A. Schnieke, G. Schneider and D. Saur, *British Journal of Cancer*, **111(5)**, 817(2014), <https://doi.org/10.1038/bjc.2014.215>
8. H. Lu and J. Martí, *The Journal of Physical Chemistry Letters*, **11(22)**, 9938(2020), <https://doi.org/10.1021/acs.jpcllett.0c02809>
9. G. Krishnamurthy, D. Roy and J. Kumar, *International Journal of Applied Pharmaceutics*, **12(5)**, 70(2020), <https://doi.org/10.22159/ijap.2020v12i5.38586>
10. J. D. Berlin, P. Catalano, J. P. Thomas, J. W. Kugler, D. G. Haller, A. B. Benson, *Journal of Clinical Oncology*, **20(15)**, 3270(2002), <https://doi.org/10.1200/jco.2002.11.149>
11. Al-Mulla, *Der Pharma Chemica*, **9(13)**, 141(2017).
12. E. A. Popova, A. V. Protas and R. E. Trifonov, *Anti-Cancer Agents in Medicinal Chemistry*, **17(14)**, 1856(2017), <https://doi.org/10.2174/1871520617666170327143148>
13. C. G. Neochoritis, T. Zhao and A. Dömling, *Chemical Reviews*, **119(3)**, 1970(2019), <https://doi.org/10.1021/acs.chemrev.8b00564>
14. M. A. Gani, A. D. Nurhan, S. Maulana, S. Siswodihardjo, D. W. Shinta and J. Khotib, *Journal of Advanced Pharmaceutical Technology & Research*, **12(2)**, 120(2021), https://doi.org/10.4103%2Fjaptr.JAPTR_88_21
15. R. Kalirajan, S. Sankar, S. Jubie and B. Gowramma, *Indian Journal of Pharmaceutical Education and Research*, **51(1)**, 110(2017).
16. X. D. Sun, X.E. Liu and D. S. Huang, *Oncology Reports*, **29(6)**, 2401(2013), <https://doi.org/10.3892/or.2013.2385>
17. A. Moulishankar and K. Lakshmanan, *Data in Brief*, **29**, 105243(2020), <https://doi.org/10.1016/j.dib.2020.105243>
18. L. Toppo, M. Yadav, S. Dhagat, S. Ayothiraman and S. E. Jujjavarapu, *Indian Journal of Biochemistry and Biophysics*, **58(2)**, 127(2021).
19. J. J. Sahayarayan, K. S. Rajan, M. Nachiappan, D. Prabhu, R. G. Rao, J. Jeyakanthan, A. H. Mahmoud, O. B. Mohammed, A.M.A. Morgan, *Saudi Journal of Biological Sciences*, **27(12)**, 3327(2020), <https://doi.org/10.1016/j.sjbs.2020.10.019>
20. J. C. Jainey, S. Priya, D. Jyothi and S. Dixit, *International Journal of Applied Pharmaceutics*, **13(6)**, 157(2021), <https://doi.org/10.22159/ijap.2021v13i6.42801>
21. K. C. Ross, A. J. Andrews, C. D. Marion, T. J. Yen and V. Bhattacharjee, *Molecular Cancer Therapeutics*, **16(8)**, 1596(2017), <https://doi.org/10.1158/1535-7163.mct-16-0798>
22. V. Subbiah, U. Lassen, E. Élez, A. Italiano, G. Curigliano, M. Javle, F. Braud, G. W. Prager, R. Greil, A. Stein, A. Fasolo, J. H. M. Schellens, P. Y. Wen, K. Viele, A.D Boran, E. Gasal, P. Burgess, P. Ilankumaran, Z. A. Wainberg, *The Lancet Oncology*, **21(9)**, 1234(2020), [https://doi.org/10.1016/s1470-2045\(20\)30321-1](https://doi.org/10.1016/s1470-2045(20)30321-1)
23. N. Awasthi, D. Kronenberger, A. Stefaniak, M. S. Hassan, U. von Holzen, M. A. Schwarz and R. E. Schwarz, *Cancer Letters*, **459**, 41(2019), <https://doi.org/10.1016/j.canlet.2019.05.037>
24. J. Sun, Z. Wan, Y. Chen, J. Xu, Z. Luo, R. A. Parise, D. Diao, P.i Ren, J.H. Beumer, B. Lu, S. Li, *Acta Biomaterialia*, **106**, 289(2020), <https://doi.org/10.1016/j.actbio.2020.01.039>
25. E. S. Knudsen, V. Kumarasamy, S. Chung, A. Ruiz, P. Vail, S. Tzetzio, J. Wu, R. Nambiar, J. Sivinski, S. S. Chauhan, M. Seshadri, S. I. Abrams, J.Wang, A.K. Witkiewicz, *Gut*, **70(1)**, 127(2021), <https://doi.org/10.1136/gutjnl-2020-321000>
26. A. B. Umar, A. Uzairu, G. A. Shallangwa and S. Uba, *SN Applied Sciences*, **2(5)**, 1(2020), <https://doi.org/10.1007/s42452-020-2620-8>
27. <https://www.sib.swiss/>
28. S. A. Attique, M. Hassan, M. Usman, R. M. Atif, S. Mahboob, K. A. Al-Ghanim, M. Bilal and N. Nawaz, *International Journal of Environmental Research and Public Health*, **16(6)**, 923(2019), <https://doi.org/10.3390%2Fijerph16060923>

29. M.R. Blessy, R.D. Patel, P.N. Prajapati and Y.K. Agrawal, *Journal of Pharmaceutical Analysis*, **4(3)**, 159(2014)
30. A.S. Nazifa, L. Mobina, M. Mehfuza, P. Seema, A. Ahmed and J. Khan, *Journal of Pharmaceutical Research International*, **33**, 254 (2021)
31. M. Abdullahi and S. E. Adenij, *Chemistry Africa*, **3**, 989(2020), <https://doi.org/10.1007/s42250-020-00162-3>
32. V. Kavitha, M. Nambiar, C. S. Ananda, B. Choudhary, K. Muniyappa, K. S. Rangappa, S.C. Raghavan, *Biochemical Pharmacology*, **77(3)**, 348(2009), <https://doi.org/10.1016/j.bcp.2008.10.018>
33. H. Lodish, A. Berk and S. L. Zipursky, 2000, Section 24.2 Proto-Oncogenes and Tumor-Suppressor Genes, *Molecular Cell Biology*, 4th Edition, W. H. Freeman, New York.
34. M. Phadke, L. L. Remsing, I. Smalley, A. T. Bryant, Y. Luo, H. R. Lawrence, B. J. Schaible, Y. A. Chen, U. Rix and K. S. Smalley, *Molecular Oncology*, **12(1)**, 74(2018), <https://doi.org/10.1002%2F1878-0261.12152>
35. J. E. Donald, D. W. Kulp and W. F. DeGrado, *Proteins: Structure, Function, and Bioinformatics*, **79(3)**, 898(2011), <https://doi.org/10.1002/prot.22927>
36. T. Infield, A. Rasouli, G. D. Galles, C. Chipot, E. Tajkhorshid, and C. A. Ahern, *Journal of Molecular Biology*, **433(17)**, 167035(2021), <https://doi.org/10.1016/j.jmb.2021.167035>
37. G. Bickerton, G. V. Paolini, J. Besnard, S. Muresan, A. L. Hopkins, *Chemistry*, **4(2)**, 90(2012), <https://doi.org/10.1038/nchem.1243>
38. M. Murahari, K. V. Prakash, G. J. Peters and Y. C. Mayur, *European Journal of Medicinal Chemistry*, **139**, 961(2017), <https://doi.org/10.1016/j.ejmech.2017.08.023>
39. M. H. Malani, B. Z. Dholakiya, A. S. Ibrahim and F. A. Badria, *Medicinal Chemistry Research*, **23(10)**, 4427(2014), <https://doi.org/10.1007/s00044-014-1010-4>
40. R. Wulandari, Sudjadi, S. Martono and A. Rohman, 2018, *Journal of Applied Pharmaceutical Science*, **8(09)**, 107(2018), <https://dx.doi.org/10.7324/JAPS.2018.8916>
41. V. H. Bhaskar and P. B. Mohite, *Journal of Optoelectronic and Biomedical Materials*, **2(4)**, 249(2010).
42. M. Nasrollahzadeh, M. Sajjadi, M. R. Tahsili, M. Shokouhimehr and R. S. Varma, *ACS Omega*, **4(5)**, 8985(2019), <https://doi.org/10.1021/acsomega.9b00800>
43. M. L. Lestari and G. Indrayanto, *Profiles of Drug Substances, Excipients and Related Methodology*, **39**, 113(2014), <https://doi.org/10.1016/B978-0-12-800173-8.00003-9>

[RJC-8114/2021]